Frequency- and time-domain femtosecond vibrational sum frequency generation from CO adsorbed on Pt(111)

W. G. Roeterdink, O. Berg, and M. Bonn

Citation: The Journal of Chemical Physics **121**, 10174 (2004); doi: 10.1063/1.1802291
View online: http://dx.doi.org/10.1063/1.1802291
View Table of Contents: http://scitation.aip.org/content/aip/journal/jcp/121/20?ver=pdfcov
Published by the AIP Publishing

Frequency- and time-domain femtosecond vibrational sum frequency generation from CO adsorbed on Pt(111)

W. G. Roeterdink and O. Berg
Leiden Institute of Chemistry, Leiden University, P.O. Box 9502, 2300 RA Leiden, The Netherlands

M. Bonn
Leiden Institute of Chemistry, Leiden University, P.O. Box 9502, 2300 RA Leiden, The Netherlands and FOM-Institute for Atomic and Molecular Physics, Kruislaan 407, 1098 SJ Amsterdam, The Netherlands

(Received 25 November 2003; accepted 9 August 2004)

We have studied the effects of intermolecular and intramolecular coupling on the C–O stretching vibration of CO adsorbed on Platinum (111) by means of femtosecond broadband vibrational sum frequency generation (VSFG). Resonant intermolecular coupling is investigated through the coverage dependence of the VSFG signal. The experimental observations can be accurately modeled as lateral coupling of the molecular transition dipole moments; this coupling is invoked in the nonlinear optical response model as a local field correction. The linear polarizability, which appears in this model, is modified by both the dipole-dipole coupling and the population of bridged adsorption sites. By extending the formalism to include these effects, we deduce a vibrational polarizability of 0.32 $Å^3$ from the data. Intramolecular coupling to the frustrated translational mode is observed as temperature dependence of the C–O stretch. The present data can be described either by pertubative or nonpertubative lineshape models from the literature. Measurements of the temperature dependence of the vibrational free induction decay indicate a population relaxation time T_1 of (0.8 ± 0.1) ps, in agreement with the observed low-temperature linewidth. Moreover, the ability of this time-domain method to discriminate spectral inhomogeneity yields clear evidence of the order-disorder transition near 275 K. Above this temperature an inhomogeneous linewidth component of (12 ± 3) cm^{-1} is observed. This value allows us to estimate the structural heterogeneity of the disordered phase, which result agrees with published Monte Carlo simulations.
 [DOI: 10.1063/1.1802291]

I. INTRODUCTION

The accumulation and dissipation of vibrational energy are central to the mechanisms of chemical catalysis. Therefore the interaction between various vibrational modes of molecular adsorbates on metals has been the subject of extensive study.[1,2] Spectroscopic methods that have been applied to this challenge include infrared absorption,[3–7] infrared pump/probe,[8–14] and infrared+visible sum frequency generation.[15–21] Such studies have established that adsorbed molecules can exchange vibrational energy by coupling of their transition dipole moments. When this dipole is large, as is often the case for chemisorbed CO, the excitation will be delocalized over several molecules. The resulting vibrational excitons have been characterized through their infrared absorption lineshape,[4–7,22,23] in conjunction with theoretical modeling of the coverage-dependent coupling,[24] and through pulsed laser saturation experiments.[9,10]

The present study concerns a benchmark system of this type: CO molecules adsorbed onto the (111) face of a single Pt crystal. We have measured the C–O stretching resonance, in both the frequency and time domains, as a function of coverage and temperature. Because the adsorption potential and the overlayer structures have been previously documented, our analysis is able to distinguish and quantify subtle influences on the lineshape: resonant intermolecular coupling, anharmonic mixing with external (librational) modes, and structural disorder.

The strength of resonant intermolecular coupling in a condensed phase (hence the extent of delocalization) depends on the oscillator strength and geometrical arrangement of molecules. When the former is expressed as (vibrational) polarizability α_v, the latter is an Ewald sum $U(0)$:[25] $U_i(0)=\Sigma_j 1/|r_i-r_j|^3$, i.e., the sum of reciprocal distances to all resonantly coupled neighbors of molecule *i*, cubed. These distances can be obtained from low-energy electron diffraction data (LEED). Coupling to image dipoles is significant on metal surfaces; this must be included in the Ewald sum,[25] at a distance that can be estimated from scanning tunneling microscopy (STM) images. For example, $U(0)$ for CO on Ru(001) is 0.17 $Å^{-3}$,[26] and for CO on Cu(100) $U(0)=0.30\,Å^{-3}$.[27] The geometric dipole sum for CO on Pt(111) was first evaluated by Crossley and King,[5] who found $U(0)=0.06\,Å^{-3}$.

In order to analyze our new sum-frequency spectra from CO/Pt(111), we extend the theory developed by Cho *et al.*[28] with the help of the model developed by Persson and Rydberg.[26] This yields a value for the vibrational polarizability of $\alpha_v=(0.32\pm0.01)\,Å^3$. We also analyze the data previously reported by Olsen and Masel,[6] Schweizer *et al.*,[7] and Klünker *et al.*,[29] resulting in $\alpha_v=0.33\,Å^3$, $\alpha_v=0.24\,Å^3$, and

$\alpha_v = 0.31\,\text{Å}^3$, respectively; the first and last are in good agreement with our findings.

Intramolecular coupling of the CO stretching vibration with low-frequency external modes gives rise to a shift of the internal vibration as a function of temperature.[7,9] This shift has been attributed to continuous thermal excitation and deexcitation of the frustrated translational mode, which is anharmonically coupled to the CO stretch: the C–O stretching frequency is modulated by lateral displacement over the platinum surface. To describe the intramolecular coupling, two exchange models have been proposed, by Persson *et al.*[24] and by Shelby *et al.*[30] We shall compare the two models and demonstrate their equivalence under specific conditions.

Finally, RAIRS and LEED data[7,31] have shown evidence for an order-disorder transition in the saturated CO/Pt(111) monolayer around $T_c = 275\,\text{K}$. The broadening of infrared absorption lines above this temperature has been attributed to increased structural inhomogeneity.[7] In the same temperature range LEED intensity deviates from the expected exponential dependence,[7] an effect also attributed to the order-disorder transition. However, the structural disorder has not been quantified. By time-domain sum frequency generation (SFG) measurements we can isolate and measure the vibrational inhomogeneity as $(12 \pm 3)\ \text{cm}^{-1}$. This, in turn, corresponds to displacement of CO molecules approximately 0.2 Å away from their low-temperature adsorption sites.

II. EXPERIMENT

We study lateral and intramolecular interactions of the CO molecules adsorbed on Pt(111) using the surface-specific technique of vibrational sum frequency generation (VSFG).[32] The VSFG experiments were performed in an ultrahigh vacuum chamber with a base pressure of 1×10^{-10} mbar. Differentially pumped CaF_2 windows serve as entrance and exit ports for the laser radiation. The platinum crystal was cleaned by sputtering with Ar^+ ions at room temperature, at a current of 3 μA/cm^2, followed by annealing to 1200 K. CO was dosed via a leak valve. Thermal desorption spectroscopy was used to determine the coverage. The saturation coverage at 273 K is assumed to be 0.5 ML, where ML represents monolayer.[33] Coverage was determined by scaling the area under the temperature programmed desorption peak. The surface was always dosed with CO at 273 K, and subsequently cooled to the desired temperature.

The light source is an amplified Ti:sapphire laser that produces 600 μJ pulses centered around 788 nm [130 fs full width at half maximum (FWHM), 1 kHz]. The major part, 500 μJ, is sent into an optical parametric amplifier (TOPAS) which produces 130 μJ of signal and idler, with the signal centered around 1353 nm. After difference mixing of signal and idler in a 2 mm AgGaS crystal, 5 μJ pulses are obtained at 4785 nm (2090 cm^{-1}), with a bandwidth of 200 cm^{-1}. The smaller part of the amplifier output is sent into a pulse shaper. The pulse shaper consists of a grating, which angularly disperses the short 788 nm pulse, a collimating lens, and a slit that reduces its spectral bandwidth. The resulting upconversion pulse has an energy of 1–2 μJ, centered at 788 nm, with a FWHM of 3.5–6.1 cm^{-1}. A cross correlation between the infrared and the upconversion pulses typically yields a transient of ~6 ps duration (FWHM), assuming Gaussian beam profiles. For time-domain experiments the slit of the pulse shaper is removed, yielding the full bandwidth of the laser pulse, which results in a cross-correlation time between the upconversion pulse and the infrared pulse of 250 fs. A 20 cm CaF_2 lens is used to focus the upconversion pulse to a 500 μm focus (Gaussian FWHM). The mid-infrared pulse is focused to a 400 μm spot. This beam is incident on the crystal at grazing incidence, and the upconversion pulse is nearly collinear. In the experiments reported here, the total fluence on the Pt(111) crystal never exceeded 2.5 mJ/cm^2. Temporal and spatial overlap are found by redirecting both beams into a $LiIO_3$ nonlinear optical crystal outside the vacuum, in which SFG is readily generated. The SFG signal is dispersed by a grating spectrometer and detected with an intensified charge coupled device camera.

III. RESULTS

VSFG spectra of the C–O stretching vibration are shown in Fig. 1 as a function of coverage, at 273 K. The resonance frequency increases from $(2083.5 \pm 0.1)\ \text{cm}^{-1}$ at 0.11 ML to $(2094.2 \pm 0.1)\ \text{cm}^{-1}$ at 0.5 ML. These frequencies are determined by fitting the spectra to a compound lineshape function, as follows.

The second-order nonlinear susceptibility $\chi^{(2)}$ is the sum of two complex amplitudes: a nonresonant electronic response (labeled nr), which duplicates the Gaussian infrared laser spectrum, and a resonant response (labeled r), which is a Lorentzian of width Γ_r centered at ω_r:

$$I_{\text{SFG}} \sim |\chi^{(2)}|^2,$$
$$\chi^{(2)} = A_{nr} e^{-[(\omega-\omega_{nr})/\Upsilon_{nr}]^2} e^{i\Phi} + \frac{A_r}{\omega - \omega_r + i\Gamma_r/2}. \tag{1}$$

A_{nr} and A_r are the amplitudes of the nonresonant and the resonant susceptibilities, respectively, and ω is the frequency of the mid-infrared light. The central frequency ω_{nr} and width Υ_{nr} of the nonresonant SFG are determined by the IR pulse properties, and can be determined independently when no CO is present on the crystal. These values are kept fixed while fitting the signals at higher coverage. The phase of the nonresonant contribution, Φ, was chosen to minimize the sum of errors in a fit to one of the low coverage spectra, and was kept fixed at this number for all other coverages. Finally, the VSFG spectra are fit to the convolution (in the frequency domain) of $\chi^{(2)}$ and the field amplitude of the upconversion pulse, which was measured separately. The fits are shown in Fig. 1 as solid lines, and the fit parameters are listed in Table I. Our data compare well with the picosecond SFG measurements of Klünker *et al.*[29] and the RAIRS measurements of Olsen and Masel;[6] the center frequencies in all cases agree to within 1 cm^{-1}.

We have measured VSFG spectra as a function of temperature at three different coverages: 0.05, 0.2, and 0.5 ML. The dispersion of the C–O stretch frequency as a function of temperature is shown in Fig. 2. The slope of our curves, $\partial\omega_r/\partial T = -0.024\,\text{cm}^{-1}/\text{K}$, is in good agreement with the

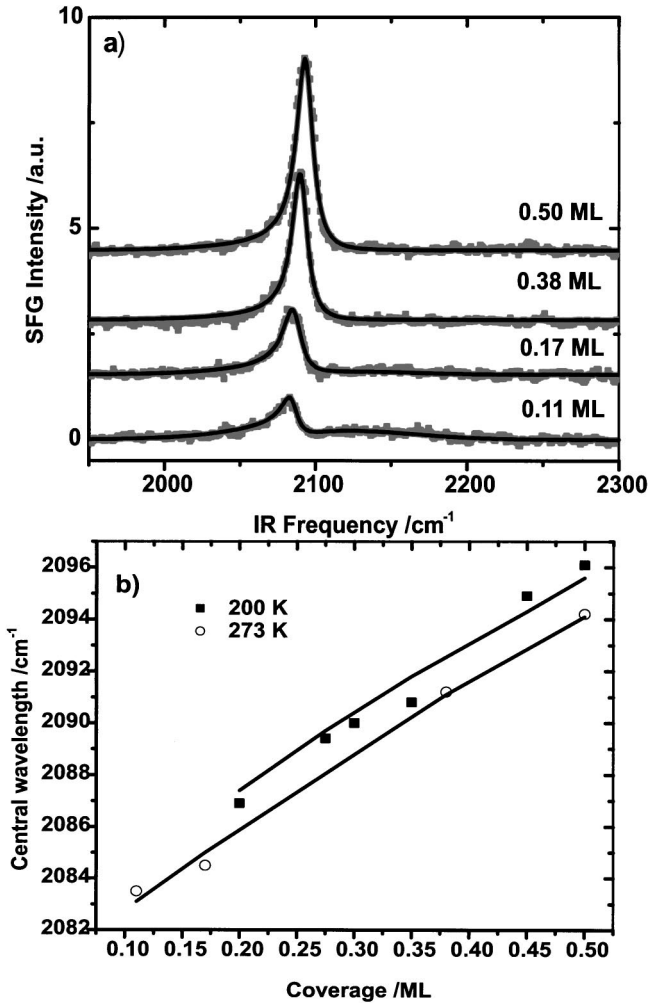

FIG. 1. (a) SFG spectra of CO at coverages indicated in the graph, recorded at 273 K. The solid lines are fits to Eq. (1). A shift in central frequency from 2094.2 to 2083.5 cm^{-1} is observed while lowering the coverage from 0.50 to 0.11 ML. (b) The solid line gives the CO stretching frequency as a function of coverage as predicted by the adapted local field model with $\alpha_v = 0.32\ Å^3$. The dots give the measured central frequencies. The points around 0.3 ML, at 200 K, are lower than the predicted values. Around 0.3 ML the overlayer slightly deviates from (4×2) structure which results in a 10% lower value for U (Ref. 31).

RAIRS measurements by Schweizer *et al.*[7] and Beckerle *et al.*[9] The linewidth of the SFG signal at saturation coverage 0.5 ML and 273 K was found to be 7 cm^{-1} FWHM (see Fig. 3), where Klünker *et al.*[29] found 10 cm^{-1}. At 0.05 ML we observe a width of (5.5±1.4) cm^{-1}, for which Klünker *et al.* found 13 cm^{-1}. We varied the energy of our infrared laser between 0.8 and 2.4 μJ and observed no effect on the linewidth of the SFG signal, indicating that saturation effects are

TABLE I. Fit parameters found for the frequency domain SFG signal at 273 K.

θ (ML)	ω_r (cm^{-1})	Linewidth (cm^{-1})
0.50	2094.2	7.1
0.38	2090.0	6.3
0.17	2084.5	8.5
0.11	2083.5	6.9

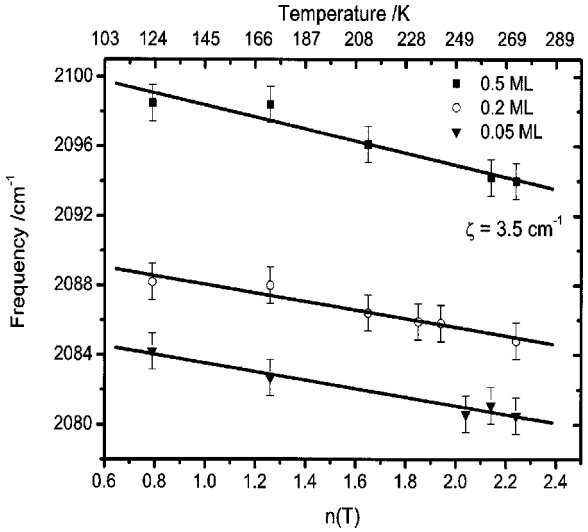

FIG. 2. The dispersion of the CO vibrational frequency plotted versus the Boltzmann factor $n(T) = 1/[\exp(hc\nu/kT) - 1]$, recorded at three different coverages. ζ is the vibration/libration coupling constant defined in the statistical theory of Persson.

negligible. The linewidths measured in our SFG experiments are in good agreement with the linewidths found in the RAIRS experiments by Schweizer *et al.*[7]

RAIRS and LEED experiments suggest that an order-disorder phase transition occurs within the CO layer near $T \approx 275\ K$.[7] Vibrational resonances should be inhomogeneously broadened in the disordered phase, but this is difficult to observe with frequency-domain measurements—whether RAIRS or SFG. But when an SFG experiment is conducted with pulses shorter than the vibrational dephasing time, it is possible to first pump the vibrations coherently, then probe the decay of material polarization (free induction decay) with a delayed upconversion pulse. Because the resonant and nonresonant contributions are separated in time,

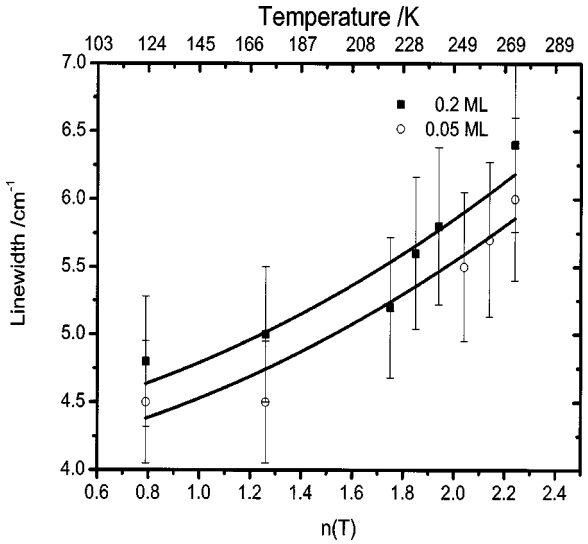

FIG. 3. Linewidth of the SFG signal as a function of temperature. The solid line is a fit with Eq. (8). The error bars indicate the standard deviation for the fitted values.

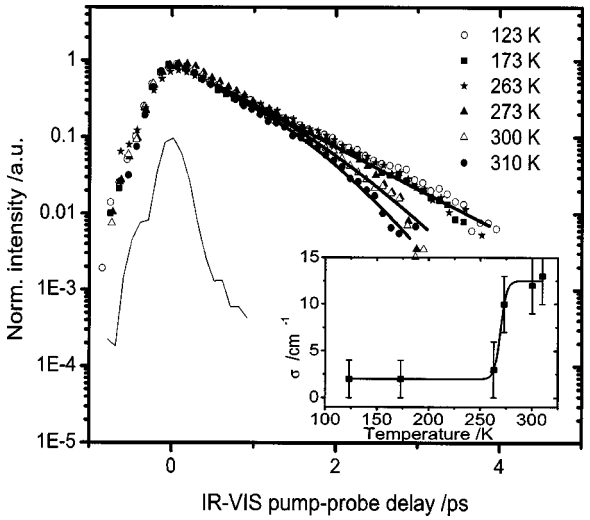

FIG. 4. SFG pump-probe transients plotted on a logarithmic scale. The deviation from the straight line is caused by inhomogeneous broadening. The nonresonant SFG signal is one order of magnitude smaller than the resonant signals and is only present around $\tau=0$. The width of the cross correlation between the infrared pulse and the visible pulse is 250 fs. Inset: The inhomogeneity as a function of temperature. At 270 K a clear jump in inhomogeneity is observed.

such measurements are better able to distinguish different line-broadening mechanisms (i.e., homogeneous versus inhomogeneous).[34]

Time-domain SFG transients for the saturated CO/Pt(111) monolayer are shown in Fig. 4 at several temperatures. Below 263 K pure exponential decay is observed, which is characteristic of homogeneous broadening. Above 263 K the distinct curvature of these semilogarithmic plots is indicative of nonexponential decay, hence inhomogeneity of the vibrational resonance. Any nonresonant contribution is limited to times around $\tau=0$, which means that at longer times the transient is determined completely by decay of the resonant polarization:[34]

$$I_{\mathrm{SFG}}(t)\sim e^{-2t/T_2}e^{-t^2\sigma^2/2}. \tag{2}$$

Here T_2 is the homogeneous dephasing time and σ is the inhomogeneous contribution to the linewidth. Fits to the data are shown as solid lines in Fig. 4, with parameters listed in Table II. Below 263 K the dephasing time T_2 is approximately 1.6 ps, with a weak temperature dependence. Above 263 K the inhomogeneous component increases abruptly, as shown in the inset of Fig. 4, and the pure dephasing time increases gradually.

TABLE II. Fit parameters found for the time domain SFG signal at 0.5 ML.

Temperature (K)	T_2 (ps)	σ (cm^{-1})
123	1.6±0.1	2±2
173	1.6±0.1	2±2
263	1.6±0.1	3±3
273	1.4±0.1	10±3
300	1.4±0.1	12±3
310	1.3±0.1	13±3

IV. DISCUSSION

A. Coverage dependence

The coverage-dependent signal can be related to intermolecular coupling through an appropriate analysis. The analysis is simplified by noting that the raw observation of a coverage-dependent resonance frequency implies a statistical occupancy of adsorption sites by CO. The data further suggest that the transition dipole moment of an individual CO molecule is independent of coverage and adsorption site; for CO/Pt(111), this is concluded from the observation that both the integrated SFG intensity and frequency are proportional to the coverage. Under these conditions, the vibrational lineshape can be related to intermolecular coupling in a relatively straightforward fashion.

Our model of the SFG lineshape will account for two coverage-dependent phenomena that have been neglected in previous treatments for SFG measurements: the effect of dipole-dipole coupling on the linear polarizability and the occupation of bridged adsorption sites (which occurs at coverages $\theta>0.33$ ML). The "local field correction" model developed by Cho *et al.*[28] can be extended to include these effects. The original model relates the intermolecular dipole-dipole coupling $U(0)$ to the SFG signal through[28]

$$I_{\mathrm{SFG}}\sim|\chi^{(2)}|^2;\qquad \chi^{(2)}=\frac{c_A\beta(\omega_{\mathrm{IR}},\omega_{\mathrm{vis}})}{[1+c_A\alpha(\omega_{\mathrm{IR}})U(0)][1+c_A\alpha_e U(0)]^2}. \tag{3}$$

$\chi^{(2)}$ is the second-order nonlinear susceptibility and c_A is the normalized coverage (i.e., at the saturation coverage 0.5 ML, $c_A=1$). The linear and the second-order polarizability $\alpha(\omega_{\mathrm{IR}})$ and $\beta(\omega_{\mathrm{IR}},\omega_{\mathrm{vis}})$ are given by

$$\alpha(\omega_{\mathrm{IR}})=\alpha_e+\frac{\alpha_v}{1-(\omega_{\mathrm{IR}}/\omega_0^2)(\omega_{\mathrm{IR}}+2i\Gamma)}, \tag{4}$$

$$\beta(\omega_{\mathrm{IR}},\omega_{\mathrm{vis}})=\beta_{\mathrm{nonres}}+\frac{\beta_{\mathrm{res}}}{1-\omega_{\mathrm{IR}}/\omega_0-i\Gamma/\omega_0}, \tag{5}$$

in which $\alpha_e=2.5\,\text{Å}^3$ (Ref. 35) is the electronic part of the linear polarizability, α_v is the vibrational part of the linear polarizability, and ω_0 and Γ are the singleton frequency and linewidth. The nonresonant part of the second-order polarizability, β_{nonres}, is set to zero.[28] However, as opposed to the Ru(001) surface,[28] on Pt(111) we must explicitly take into account that the polarizability is altered by occupation of different surface sites for coverages greater than $\theta=0.33$ ML.[26] Instead of using Eq. (4), the linear polarizability should therefore be calculated using[26]

$$\alpha(\omega_{\mathrm{IR}})=\sum_{\mu=1}^{M}\frac{c_\mu\alpha_\mu(\omega_{\mathrm{IR}})}{1+[\alpha_\mu(\omega_{\mathrm{IR}})-\alpha(\omega_{\mathrm{IR}})]Q}, \tag{6}$$

in which α_μ is calculated with Eq. (4) for one of the specific binding sites μ (bridged or atop). c_μ is the normalized population and Q is an analytical transendental function of α and $U(0)$,[26] taken from the theory by Persson and Rydberg, which describes how the dipole-dipole coupling can be deduced from RAIRS data.[26] Equation (6) must be solved nu-

merically in a self-consistent manner. The resultant value of $\alpha(\omega_{IR})$ is then used in Eq. (3) to calculate the SFG signal. The influence of dipole-dipole coupling on the linear polarizability, and the adsorption of CO at bridged sites at coverages above 0.33 ML are thereby incorporated in the local field correction. The dipole-dipole coupling $U(0)$ can be evaluated using the Ewald sums given by Scheffler.[25] Counting only the atop molecules and their image dipoles, a coupling of 0.1 $Å^{-3}$ is found. Specifically, the interaction with other dipoles contributes 0.06 $Å^{-3}$, and the interaction with other images 0.04 $Å^{-3}$. The distance from the image plane to the CO molecule was deduced from STM data of Pedersen *et al.*,[36] within a jellium model,[37] to be 0.8 Å, which is similar to the value for CO on Pd(110).[38] (The dipole-dipole coupling strength is highly sensitive to the postulated distance between the image plane and the molecule, which explains the different value obtained by Crossley and King, 0.057 $Å^{-3}$.[35]) Finally, the vibrational polarizability is used as a parameter to fit Eq. (3) to our data. The fits shown in Fig. 1 yield a value of $\alpha_v = 0.32\ Å^3$. We have applied the same analysis to the isotopic dilution data published by Olsen and Masel[6] and Schweizer *et al.*,[7] using the collective mode model developed by Persson and Rydberg.[26] It clearly shows that there is a discrepancy between the vibrational polarizability derived from Schweizer's IR data,[7] $\alpha_v = 0.24\ Å^3$ and from Olsen's IR data,[6] $\alpha_v = 0.33\ Å^3$. Our value of $\alpha_v = (0.32 \pm 0.01)\ Å^3$ agrees well with the latter. Equations (3) and (4) show that the SFG intensity depends on the inverse of α_v. The integrated RAIRS intensity, on the other hand, is directly proportional to α_v. That one value for the resonant polarizability can reproduce both data sets indicates that the model is internally consistent.

B. Temperature dependence

The shift and broadening of the vibrational line with temperature (Figs. 2 and 3) have been attributed to continuous thermal excitation and deexcitation of the low-frequency frustrated translational mode. The C–O stretching frequency is modulated by these small, reversible lateral displacements over the platinum surface;[7,9] this effect enters the formalism as an anharmonic coupling term. We shall discuss two detailed models of the C–O stretching lineshape that include such coupling: a statistical model, developed by Persson *et al.*,[24] which is pertubative; and an essentially nonpertubative exchange model describing developed by Shelby *et al.*[30] It will be shown that the two models give the same coupling constant, indicating that a pertubative treatment is sufficient.

The statistical model is based on classical mechanics, so the CO molecules are described as forced harmonic oscillators. In the set of coupled equations of motion, the variance of the low frequency mode $\langle Q^2 \rangle$ is added to the diagonal elements as a perturbation. The variance is calculated assuming a Markovian process for the thermal excitation and deexcitation of the frustrated translation. The frequency and width of the C–O stretching vibration, both at constant coverage, are then given by[24]

$$\nu = \nu_0 - \xi n(T), \tag{7}$$

$$\delta\nu = \delta\nu_0 + \frac{2\xi^2}{\eta} n(T)[n(T)+1], \tag{8}$$

in which ν_0 is the central frequency at 0 K, ξ is a measure of the coupling strength, $n(T) = 1/[\exp(hc\nu_{LF}/kT) - 1]$ is the Bose–Einstein factor, and $\delta\nu_0 \sim 1/T_2$ is the linewidth at 0 K (with effective dephasing time T_2). η is the linewidth of the low-frequency frustrated translational mode.

A different model was developed by Shelby *et al.* to describe the dephasing of vibrations in polyatomic molecules.[30] In this model the density matrix method is applied to a four-level system, with two levels for the CO stretching vibration and two levels for the anharmonically coupled low-frequency mode—in this case the frustrated translation ν_4. The off-diagonal coupling terms are given by the thermal excitation and deexcitation rate of the frustrated translation. The resulting frequency of the internal mode is equivalent to Eq. (7), with

$$\xi = \frac{\gamma^2 \zeta}{\gamma^2 + \zeta^2}, \tag{9}$$

where $\gamma \sim 1/T_1^{LF}$ is the inverse lifetime of the low-frequency mode and ζ is the vibration/libration coupling constant.

Although the two models differ in their treatment of the coupling between the high- and low-frequency modes, both models require the frequency of the latter. There has been some debate about the exact frequency of the external modes for the CO/Pt(111) system[39–41] and the assignments are not consistent throughout the literature. We follow the original paper of Richardson and Bradshaw,[42] in which ν_4 is assigned to the lateral frustrated translation. The only direct observation of this mode is by Lahee *et al.*, who measured a frequency of 60 cm^{-1} by He scattering.[43]

Following the model developed by Persson *et al.*,[24] we have fit the temperature dependence of the central frequency to Eq. (7). At saturation coverage a value of 3.5 cm^{-1} is found for ξ. At lower coverage the slope of the line (see Fig. 2), which reflects the strength of coupling to the frustrated translation, is found to be smaller. This change can be attributed either to a change in coupling constant ξ with coverage, or to a change in frequency of the frustrated translation ν_4, which would make $n(T) = 1/[\exp(hc\nu_4/kT) - 1]$ coverage dependent [Eq. (7)]. Schweizer *et al.* have also observed this, and have invoked the latter explanation to account for their data.[7]

Assuming that the factor $\xi = 3.5\ cm^{-1}$ is independent of coverage, our data in Fig. 2 show that the frequency of the frustrated translation decreases from 60 cm^{-1} at 0.5 ML to 51 cm^{-1} below 0.2 ML. This is in good agreement with inelastic helium scattering experiments by Lahee *et al.*, who observed a decrease from 60 to 49 cm^{-1} with decreasing coverage.[43] Schweizer *et al.* attributed this change to the interaction of atop-bound CO with bridge-bound CO. Below 0.33 ML no bridged sites are occupied, so the frequency of the frustrated translation should be unaffected, as we observe.

To describe the temperature dependence of the SFG linewidths, Eq. (8) is used. The fits to our data are shown in Fig. 3. At 0.2 ML, we find $\delta\nu_0 = 4.3 \pm 0.2\ cm^{-1}$ and $\eta = 88 \pm 11$

cm^{-1}, while at 0.05 ML $\delta\nu_0 = 3.2 \pm 0.4\,cm^{-1}$ and $\eta = 53 \pm 6$ cm^{-1}. Our linewidth measurements are further corroborated by our time-domain experiments. To determine the dephasing time, Eq. (2) has been fit to the time-domain SFG spectra. The results are listed in Table II. We can derive the population relaxation time from these data by extrapolating the temperature-dependent dephasing time to 0 K, for which Eq. (8) is used. Note that at $T = 0$ K, $T_2 = 2T_1$. The tentative value thus obtained is (0.8 ± 0.1) ps, which is appreciably lower than the value of (2.2 ± 0.4) ps obtained by Cavanagh *et al.* by means of transient infrared absorption spectroscopy.[44] The origin of this discrepancy is not clear to us, but the derived population decay time is consistent with our frequency-domain linewidth measurements and previous RAIRS measurements,[7] which both give (0.7 ± 0.2) ps.

The two models of internal/external mode coupling are formally equivalent in the limit that the external mode's lifetime is short. Specifically, when its inverse lifetime is much larger than the internal/external coupling constant ($\gamma = 1/T_1^{\mathrm{LF}} \approx \eta \gg \zeta$), Eq. (9) reduces to $\xi = \zeta$.

C. Order-disorder transition

It has previously been observed that near 275 K the infrared absorption lines broaden due to an order/disorder transition in the saturated monolayer.[7] However, in both RAIRS and frequency-domain SFG experiments, it is very difficult to see the subtle change from a Lorentzian to a Voigt lineshape. It has been shown[34] that time-domain experiments are more sensitive in this respect, allowing for a more reliable determination of the dephasing mechanism and rate.

Indeed, our time-domain data reveal obvious nonexponential behavior at 273 K and above (see Fig. 4), which is direct evidence for inhomogeneous broadening. An inhomogeneous width of the CO stretch vibration of $\sigma = (10 \pm 3)$ cm^{-1} at 273 K is found by fitting Eq. (2) to the time-domain SFG transients shown in Fig. 4. There are no indications that the inhomogeneity below 273 K is greater than 3 cm^{-1}. The linewidths derived from our frequency-domain SFG experiments corroborate this conclusion. The temperature dependence of the inhomogeneity is summarized in the inset of Fig. 4.

The phase behavior of the CO/Pt(111) system has been discussed in detail by Persson.[45] Briefly, there are two competing influences on the molecular adsorption geometry: corrugation of the adsorbate/substrate potential and lateral repulsion between adsorbates. With increasing temperature a secondary, metastable adsorption site (atop a Pt atom with occupied nearest neighbors) becomes thermally accessible; however, occupation of this site modifies the neighboring adsorbates (also atop Pt atoms) by intermolecular repulsion. The result is a well-defined phase transition temperature, above which the molecules are displaced from their high-symmetry adsorption sites and tilted away from the surface normal. Because the energy barrier between sites is comparable to the intermolecular repulsion, the high-temperature phase is translationally disordered. The published simulations of this structure predict a range of displacements and tilts, typically 0.11 Å and 10°.

The lineshape models developed above allow us to estimate the magnitude of structural heterogeneity in the disordered phase. Structural disorder will affect both the intra and intermolecular couplings. For the latter case we can again compute an Ewald sum, $U_i(0) = \Sigma_j \cos(\theta_{ij})/|r_i - r_j|^3$, with positional and orientational disorder introduced. The result is naturally insensitive to small deviations from $\theta_{ij} = 0$, while positional displacements of tenths of angstrom change the resonance by tenths of cm^{-1}. If the observed broadening of 12 cm^{-1} were the result of structural disorder on the excitonic coupling, it would demand displacements on the order of 10 Å, which is unphysically large.

As changes in the intermolecular interactions can therefore clearly not account for the spectral changes, their origin must lie in the intramolecular effects. Indeed, the displacement of an adsorbed CO molecule away from the high-symmetry atop site, results in a weakening of its internal bond, lowering the resonance frequency.[7,9] This shift can be observed in Fig. 2, in which the displacement is caused by thermal motion of a translationally ordered layer. The magnitude of lateral displacement can be approximated by treating the external mode as a quantum harmonic oscillator. In state n, its root mean square (rms) displacement along coordinate x is $\langle x^2 \rangle^{1/2} = \sqrt{\hbar}(n + 1/2)/(2\pi m c \nu)$, where m is the mass, ν the resonance frequency, and c the speed of light. The fractional population of such an oscillator at temperature T is

$$P_n = \frac{\exp[-n\nu/(kT)]}{1 - \exp[-n\nu/(kT)]}.$$

By weighting each rms displacement by its fractional population and summing over all occupied levels, we compute the thermal average displacement $\langle\langle x \rangle\rangle = \Sigma_{n=0}^{\infty} P_n \langle x^2 \rangle^{1/2}$. The frequency of the frustrated translational mode has been measured by Lahee as 60 cm^{-1}.[44] Our measurements of the internal C–O mode range from 124 K, where $\langle\langle x \rangle\rangle = 0.16$ Å, to 280 K, where $\langle\langle x \rangle\rangle = 0.23$ Å; the corresponding spectral shift is 5 cm^{-1} (Fig. 2). Under the assumption that this is purely translation-induced chemical shift, the displacement is therefore 0.014 Å cm^{-1}. Molecules with a chemical shift of 12 cm^{-1}—characteristic of spectral inhomogeneity in the disordered phase—are therefore displaced by 0.2 Å from the atop position. This estimate agrees with the ''several tenths'' of angstrom observed by Persson in a Monte Carlo simulation of the disordered phase.[45] The chemical shift is evidently more sensitive to molecular displacement than is the intermolecular coupling; therefore the spectral inhomogeneity observed in the disordered phase is principally of chemical origin.

The spectral heterogeneity appears abruptly and levels off within 20 K, as shown in the inset of Fig. 4, suggesting the structural discontinuity of a first-order phase transition. This is in contrast with the gradually decreasing rate of bridged site occupation observed by Schweizer *et al.*[7] as temperature increased over hundreds of kelvin. The analysis by Persson and Rydberg shows that the order of the phase transition is directly connected to the anharmonicity of the frustrated translational mode;[26] when calibrated with Schweizer's data, this fourth-order anharmonicity has a value

of 2.61 $Å^{-2}$, which would yield a structurally gradual second-order transition. It is to be hoped that more detailed probes of the overlayer structure, as attempted here, will further resolve the phase behavior of this system.

V. CONCLUSION

We have investigated the vibrational dynamics of CO/Pt(111) using frequency- and time-resolved broadband SFG. A vibrational polarizability of $\alpha_v = (0.32 \pm 0.01)\ Å^3$ is found using the local field correction method for SFG data. This value is in agreement with the value derived from linear infrared spectrometry by Olsen *et al.* ($\alpha_v = 0.33\ Å^3$). The dispersion of the C–O stretch frequency with temperature is consistent with previous linear infrared measurements, and results in a coupling constant of $\xi = (3.5 \pm 0.3)\ cm^{-1}$ with the frustrated translation, in good agreement with the value obtained in RAIRS experiments ($3.3\ cm^{-1}$). We find a population relaxation time T_1 of (0.8 ± 0.1) ps, in contrast to previous transient absorption measurements ($T_1 = 2.2$ ps). An order-disorder transition is observed at 275 K, above which an inhomogeneous broadening $\sigma = (12 \pm 3)\ cm^{-1}$ is found, in agreement with Monte Carlo simulations.

ACKNOWLEDGMENTS

The authors gratefully acknowledge the excellent technical support of R. C. V. van Schie and P. Schakel. Professor A. W. Kleyn is acknowledged for helpful discussions. Dr. L. B. F. Juurlink and Dr. J. F. M. Aarts are acknowledged for their expert help with the vacuum system.

[1] R. R. Cavanagh, D. S. King, J. C. Stephenson, and T. F. Heinz, J. Phys. Chem. **97**, 786 (1993).
[2] P. Dumas, M. K. Weldon, Y. J. Chabal, and G. P. Williams, Surf. Rev. Lett. **6**, 225 (1999).
[3] H. Pfnür, D. Menzel, F. M. Hoffmann, A. Ortega, and A. M. Bradshaw, Surf. Sci. **93**, 431 (1980).
[4] P. Jakob and B. N. J. Persson, Phys. Rev. B **56**, 10644 (1997).
[5] A. Crossley and D. A. King, Surf. Sci. **68**, 528 (1977).
[6] C. W. Olsen and R. I. Masel, Surf. Sci. **201**, 444 (1988).
[7] E. Schweizer, B. N. J. Persson, M. Tüshaus, D. Hoge, and A. M. Bradshaw, Surf. Sci. **213**, 49 (1989).
[8] K. Kuhnke, M. Morin, P. Jakob, N. J. Levinos, Y. J. Chabal, and A. L. Harris, J. Chem. Phys. **99**, 6114 (1993).
[9] J. D. Beckerle, R. R. Cavanagh, M. P. Casassa, E. J. Heilweil, and J. C. Stephenson, J. Chem. Phys. **95**, 5403 (1991).
[10] Ch. Hess, M. Wolf, and M. Bonn, Phys. Rev. Lett. **85**, 4341 (2000).
[11] A. Bandara, J. Kubota, K. Onda, A. Wada, S. Kano, K. Domen, and C. Hirose, Surf. Sci. **427**, 331 (1999).
[12] P. Guyot-Sionnest, Phys. Rev. Lett. **67**, 2323 (1991).
[13] P. Guyot-Sionnest, P. H. Lin, and E. M. Hiller, J. Chem. Phys. **102**, 4269 (1995).
[14] R. P. Chin, X. Blase, Y. R. Shen, and S. G. Louie, Europhys. Lett. **30**, 399 (1995).
[15] M. Bonn, C. Hess, and M. Wolf, J. Chem. Phys. **115**, 7725 (2001).
[16] J. P. R. Symonds, H. Arnolds, V. L. Zhang, K. Fukutani, and D. A. King, J. Chem. Phys. **120**, 7158 (2004).
[17] M. Morkel, G. Rupprechter, and H.-J. Freund, J. Chem. Phys. **119**, 10853 (2003).
[18] H. Härle, K. Mendel, U. Metka, H.-R. Volpp, L. Willms, and J. Wolfrum, Chem. Phys. Lett. **279**, 275 (1997).
[19] S. Baldelli, N. Markovic, P. Ross, Y. R. Shen, and G. Somorjai, J. Phys. Chem. B **103**, 8920 (1999).
[20] X. Su, P. S. Cremer, Y. R. Shen, and G. A. Somorjai, J. Am. Chem. Soc. **119**, 3994 (1997).
[21] G. A. Somorjai and G. Rupprechter, J. Phys. Chem. B **103**, 1623 (1999).
[22] R. J. Mukerji, A. S. Bolina, and W. A. Brown, Surf. Sci. **527**, 198 (2003).
[23] M. W. Severson, C. Stuhlmann, I. Villegas, and M. J. Weaver, J. Chem. Phys. **103**, 9832 (1995).
[24] B. N. J. Persson, F. M. Hoffmann, and R. Ryberg, Phys. Rev. B **34**, 2266 (1986).
[25] M. Scheffler, Surf. Sci. **81**, 562 (1979).
[26] B. N. J. Persson and R. Ryberg, Phys. Rev. B **24**, 6954 (1981).
[27] R. Ryberg, Surf. Sci. **114**, 627 (1982).
[28] M. Cho, C. Hess, and M. Bonn, Phys. Rev. B **65**, 205423 (2002).
[29] C. Klünker, M. Balden, S. Lehwald, and W. Daum, Surf. Sci. **360**, 104 (1996).
[30] R. M. Shelby, C. B. Harris, and P. A. Cornelius, J. Chem. Phys. **70**, 34 (1979).
[31] B. N. J. Persson and R. Ryberg, Phys. Rev. B **40**, 10273 (1989).
[32] Y. R. Shen, Nature (London) **337**, 519 (1989).
[33] H. Steininger, S. Lehwald, and H. Ibach, Surf. Sci. **123**, 264 (1982).
[34] S. Roke, A. W. Kleyn, and M. Bonn, Chem. Phys. Lett. **370**, 227 (2003).
[35] A. Crossley and D. A. King, Surf. Sci. **95**, 131 (1980).
[36] M. Ø. Pedersen, M.-L. Bocquet, P. Sautet, E. Lægsgaard, and F. Besenbacher, Chem. Phys. Lett. **299**, 403 (1999).
[37] B. N. J. Persson and A. Liebsch, Surf. Sci. **110**, 356 (1981).
[38] H. Kato, H. Okuyama, S. Ichihara, M. Kawai, and J. Yoshinobu, J. Chem. Phys. **112**, 1925 (2000).
[39] U. Engström and R. Ryberg, J. Chem. Phys. **112**, 1959 (2000).
[40] U. Engström and R. Ryberg, Phys. Rev. Lett. **78**, 1944 (1997), and references therein.
[41] M. Surman, P. L. Hagans, N. E. Wilson, C. J. Baily, and A. E. Russell, Surf. Sci. **511**, L303 (2002).
[42] N. V. Richardson and A. M. Bradshaw, Surf. Sci. **88**, 255 (1979).
[43] A. M. Lahee, J. P. Toennies, and Ch. Wöll, Surf. Sci. **177**, 371 (1986).
[44] R. R. Cavanagh, J. D. Beckerle, M. P. Casassa, E. J. Heilweil, and J. C. Stephenson, Surf. Sci. **269/270**, 113 (1992).
[45] B. N. J. Persson, Phys. Rev. B **40**, 7115 (1989).